# Synthesis and Characterization of Hydroxo-Bridged Diiron(III) Complexes Containing Carboxylate or Phosphate Ester Bridges: Comparisons to Diiron(III) Proteins

**Petra N. Turowski, William H. Armstrong, Shuncheng Liu, Seth N. Brown, and Stephen J. Lippard***

Department of Chemistry, Massachusetts Institute of Technology, Cambridge, Massachusetts 02139

*Received June 30, 1993*®

Complexes containing a phosphate- or acetate-bridged ($\mu$-hydroxo)diiron(III) core, such as may exist in the metalloproteins uteroferrin, beef spleen purple acid phosphatase, or the hydroxylase component of methane monooxygenase, have been prepared. A general procedure is presented for synthesizing hydroxo-bridged complexes by protonation of their oxo-bridged analogues in ether solution. As a result of protonating the bridging oxygen atom, the dimetallic core in the hydroxo-bridged complexes is expanded (Fe–OH = 1.95–1.97 Å, Fe···Fe = 3.44–3.59 Å, ∠Fe–OH–Fe = 123–131°) relative to that in the corresponding $\mu$-oxo complexes (Fe–O = 1.78–1.81 Å, Fe···Fe = 3.10–3.33 Å, ∠Fe–O–Fe = 120–130°), with a concomitant decrease in the magnitude of the antiferromagnetic spin exchange coupling constants ($J \approx -10$ to $-20$ cm$^{-1}$) and correspondingly larger paramagnetic shifts (–20 to –70 ppm) in the $^1$H NMR spectra. Electronic transitions differ considerably from those of oxo-bridged complexes, and Mössbauer quadrupolar coupling parameters (0.25–0.40 mm/s) are considerably smaller in the hydroxo-bridged analogues. A new diiron(III) complex containing three bidentate bridging groups, $[Fe_2\{O_2P(OC_6H_5)_2\}_3(HBpz_3)_2](BF_4)$, was also prepared and characterized spectroscopically, magnetically, and structurally. In this weakly antiferromagnetically coupled compound ($J = -0.8$ cm$^{-1}$), the Fe···Fe distance is 4.677(1) Å. Unit cell data: $[Fe_2(OH)(O_2CCH_3)_2(HBpz_3)_2](ClO_4)\cdot CH_2Cl_2$, space group $C^5_{2h}$-$P2_1/n$, $a = 11.757(2)$ Å, $b = 19.925(4)$ Å, $c = 15.580(2)$ Å, $\beta = 92.03(1)°$, $V = 3647(2)$ Å$^3$, $Z = 4$, $T = -15$ °C; $[Fe_2(OH)\{O_2P(OC_6H_5)_2\}_2(HBpz_3)_2](BF_4)\cdot 2CH_2Cl_2\cdot 0.5(CH_3CH_2)_2O\cdot H_2O$, space group $C^6_{2h}$-$C2/c$, $a = 21.156(4)$ Å, $b = 20.518(2)$ Å, $c = 27.157(4)$ Å, $\beta = 104.268(7)°$, $V = 11\,425(3)$ Å$^3$, $Z = 8$, $T = -38$ °C; $[Fe_2(OH)\{O_2P(C_6H_5)_2\}_2(HBpz_3)_2](BF_4)\cdot 2.5(CH_3)_2CO$, space group $C^3_{2h}$-$C2/m$, $a = 16.772(2)$ Å, $b = 33.585(4)$ Å, $c = 10.902(1)$ Å, $\beta = 105.206(8)°$, $V = 5926(2)$ Å$^3$, $Z = 4$, $T = -54$ °C; $[Fe_2\{O_2P(OC_6H_5)_2\}_3(HBpz_3)_2](BF_4)\cdot CH_2Cl_2$, space group $C^1_i$-$P\bar{1}$, $a = 12.346(2)$ Å, $b = 15.084(2)$ Å, $c = 17.633(2)$ Å, $\alpha = 97.50(1)°$, $\beta = 99.02(1)°$, $\gamma = 95.76(1)°$, $V = 3191(2)$ Å$^3$, $Z = 2$, $T = -54$ °C.

As part of a continuing investigation of biologically relevant non-heme diiron(III) centers,[1,2] we have undertaken the study of hydroxo-bridged complexes with additional carboxylate or phosphate[3] bridging ligands. Such cores may be present in purple acid phosphatase isolated from bovine spleen[4-7] and in the homologous protein obtained from the uterine fluid of pregnant sows, uteroferrin.[8-13] Recent extended X-ray absorption fine structure spectroscopy (EXAFS)[14] and electron nuclear double resonance (ENDOR)[15] spectroscopic results on the hydroxylase component of methane monooxygenase (MMO), which catalyzes methane oxidation in methanotrophic bacteria, suggest that the two iron atoms in this enzyme are also bridged by a hydroxide ligand. The iron–iron distances in the diiron(III) forms of these proteins, determined by EXAFS, are between 3.0 and 3.45 Å. The shortest iron–ligand distance observed in each case is ~1.98 Å. These structural parameters are consistent with dinuclear Fe–OH–Fe units containing additional bridging ligands. Phosphate ligands are of interest in this chemistry because inorganic phosphate is a competitive inhibitor of purple acid phosphatase and uteroferrin, and EXAFS results indicate that the iron atoms are bridged by phosphate ligands in the phosphate-bound forms of both proteins.[4-13] Bridging carboxylates may also be present, since these groups are known to occur in proteins containing oxo-bridged diiron(III) centers, specifically hemerythrin and ribonucleotide reductase,[1,12] as well as the MMO hydroxylase.[16]

Two types of hydroxide-bridged non-heme diiron(III) complexes have been known previously, dihydroxide-bridged species[17-22] and compounds containing both a hydroxide and an aryloxide bridge.[23-26] The two monoatomic bridging groups in this class of compounds result in iron–iron distances near 3.1 Å. The complexes described in the present paper represent another class,

® Abstract published in *Advance ACS Abstracts*, December 15, 1993.

(1) Lippard, S. J. *Angew. Chem., Int. Ed. Engl.* **1988**, *27*, 344–361.
(2) Taft, K. L.; Masschelein, A.; Liu, S.; Lippard, S. J.; Garfinkel-Shweky, D.; Bino, A. *Inorg. Chim. Acta* **1992**, *198–200*, 627.
(3) Phosphate, as used here, includes phosphates, phosphonates, phosphinates, and their esters.
(4) Averill, B. A.; Davis, J. C.; Burman, S.; Zirino, T.; Sanders-Loehr, J.; Loehr, T. M.; Sage, J. T.; Debrunner, P. G. *J. Am. Chem. Soc.* **1987**, *109*, 3760–3767.
(5) Kauzlarich, S. M.; Teo, B. K.; Zirino, T.; Burman, S.; Davis, J. C.; Averill, B. A. *Inorg. Chem.* **1986**, *25*, 2781–2785.
(6) Doi, K.; Antanaitis, B. C.; Aisen, P. *Struct. Bonding* **1988**, *70*, 1–26.
(7) Davis, J. C.; Lin, S. S.; Averill, B. A. *Biochemistry* **1981**, *20*, 4062–4067.
(8) Pyrz, J. W.; Sage, J. T.; Debrunner, P. G.; Que, L. *J. Biol. Chem.* **1986**, *261*, 11015–11020.
(9) Sinn, E.; O'Connor, C. J.; de Jersey, J.; Zerner, B. *Inorg. Chim. Acta* **1983**, *78*, L13–L15.
(10) Debrunner, P. G.; Hendrich, M. P.; de Jersey, J.; Keogh, D. T.; Zerner, B. *Biochim. Biophys. Acta* **1983**, *745*, 103–106.
(11) Antanaitis, B. C.; Aisen, P.; Lilienthal, H. R. *J. Biol. Chem.* **1983**, *258*, 3166–3172.
(12) Que, L., Jr.; Scarrow, R. C. In *Metal Clusters in Proteins*; Que, L., Jr., Ed.; American Chemical Society: Washington, DC, 1988; pp 152–178.
(13) True, A. E.; Scarrow, R. C.; Randall, C. R.; Holz, R. C.; Que, L., Jr. *J. Am. Chem. Soc.* **1993**, *115*, 4246–4255.
(14) DeWitt, J. G.; Bentsen, J. G.; Rosenzweig, A. C.; Hedman, B.; Green, J.; Pilkington, S.; Papaefthymiou, G. C.; Dalton, H.; Hodgson, K. O.; Lippard, S. J. *J. Am. Chem. Soc.* **1991**, *113*, 9219–9235.
(15) De Rose, V. J.; Liu, K. E.; Kurtz, D. M., Jr.; Hoffman, B. M.; Lippard, S. J. *J. Am. Chem. Soc.* **1993**, *115*, 6440–6441.
(16) Rosenzweig, A. C.; Frederick, C. A.; Lippard, S. J.; Nordlund, P. *Nature* **1993**, *366*, 537–543.
(17) Kurtz, D. M., Jr. *Chem. Rev.* **1990**, *90*, 585–606.
(18) Wu, F.-J.; Kurtz, D. M., Jr.; Hagen, K. S.; Nyman, P. D.; Debrunner, P. G.; Vankai, V. A. *Inorg. Chem.* **1990**, *29*, 5174–5183.
(19) Vankai, V. A.; Newton, M. G.; Kurtz, D. M., Jr. *Inorg. Chem.* **1992**, *31*, 341–343.
(20) Ou, C. C.; Lalancette, R. A.; Potenza, J. A.; Schugar, H. J. *J. Am. Chem. Soc.* **1978**, *100*, 2053–2057.
(21) Thich, J. A.; Ou, C. C.; Powers, D.; Vasiliou, B.; Mastropaolo, D.; Potenza, J. A.; Schugar, H. J. *J. Am. Chem. Soc.* **1976**, *98*, 1425–1433.
(22) Borer, L.; Thalken, L.; Ceccarelli, C.; Glick, M.; Zhang, J. H.; Reiff, W. M. *Inorg. Chem.* **1983**, *22*, 1719–1724.

0020-1669/94/1333-0636$04.50/0 

($\mu$-hydroxo)diiron(III) species with bidentate bridging groups as supporting ligands. Non-heme diiron(III) compounds containing only one hydroxide bridge, other than the title compounds, have not been structurally characterized, although spectroscopic investigations of similar molecules have been carried out.[18,27] Preliminary results for the ($\mu$-hydroxo)bis($\mu$-acetato)diiron(III) complex $[Fe_2(OH)(O_2CCH_3)_2(HBpz_3)_2](ClO_4)$ (**1**), where $HBpz_3^-$ is hydrotris(1-pyrazolyl)borate, have been reported previously.[28] A related linear trinuclear complex, $[Fe_3(\mu\text{-}OH)_2(\mu\text{-}O_2CC_6H_5)_4(N3)_2](PF_6)_3$, where N3 is tris(1,4-dimethylimidazol-2-yl)phosphine, was crystallographically characterized recently.[19] The first example of a hydroxo-bridged diiron(III) heme complex has been reported.[29]

In undertaking the present investigation, we were interested in the following questions. Do hydroxo-bridged diiron(III) complexes have characteristic spectroscopic features and how do they differ from oxo-bridged analogues? How do hydroxo-bridged complexes with various additional bridging ligands differ from one another? And finally, how do the spectroscopic features of these hydroxo-bridged complexes compare with those of the proteins? To augment our understanding of hydroxo-bridged diiron(III) complexes, particularly those with phosphate ligands, we here describe the synthesis of **1**,[28] $[Fe_2(OH)\{O_2P(OC_6H_5)_2\}_2(HBpz_3)_2](BF_4)$ (**2**), and $[Fe_2(OH)\{O_2P(C_6H_5)_2\}_2(HBpz_3)_2](BF_4)$ (**3**), as well as of the tris(phosphate)-bridged complex $[Fe_2\{O_2P(OC_6H_5)_2\}_3(HBpz_3)_2](BF_4)$ (**4**), obtained for comparison with the hydroxo-bridged complexes. Full details of the characterization of these complexes by crystallographic methods and by Mössbauer, NMR, vibrational, and UV/vis spectroscopy are presented. The electrochemistry, magnetic susceptibility, and EPR spectra of the complexes are also described. The properties are compared to those of other hydroxo- or oxo-bridged complexes, as well as to uteroferrin, purple acid phosphatase, and the hydroxylase component of methane monooxygenase.

## Experimental Section

**Materials and Methods.** $[Fe_2O(O_2CCH_3)_2(HBpz_3)_2]$ (**5**),[30] $[Fe_2O\{O_2P(OC_6H_5)_2\}_2(HBpz_3)_2]$,[31,32] and $[Fe_2O\{O_2P(C_6H_5)_2\}_2(HBpz_3)_2]$,[31] where $HBpz_3^-$ is hydrotris(1-pyrazolyl)borate, were prepared as previously described. For cyclic voltammetry experiments, solvents and electrolytes were of electrochemistry grade or purified by distillation or recrystallization, respectively, prior to their use. All other reagents were obtained from commercial sources and used as supplied. Elemental analyses were performed by Atlantic Microlab, Norcross, GA, and by Galbraith Laboratories, Knoxville, TN. Mössbauer spectra of powdered samples dispersed in boron nitride were recorded at the Francis Bitter National Magnet Laboratory on a constant acceleration spectrometer with a $^{57}Co$ source in a Rh matrix. Isomer shifts are reported relative to Fe metal. $^1H$ and $^{31}P$ NMR spectra and $T_1$ measurements were obtained on a Varian XL 300 instrument using tetramethylsilane or 80% $H_3PO_4$ as reference standard. Unless otherwise specified, all NMR experiments were carried out at room temperature in $CDCl_3$, except for $T_1$ studies, which were performed in $CD_2Cl_2$. X-band EPR spectra of frozen $CH_2Cl_2$/toluene glasses (1:2) were obtained on a Bruker ESP 300 instrument and calibrated against $MnSO_4$. Fast-atom-bombardment (FAB) mass spectra in glycerol matrices were recorded on a Finnigan MAT System 8200 instrument equipped with an FAB gun using Xe atoms as the source. Ultraviolet and visible spectra were obtained on a Perkin-Elmer Lambda 7 instrument, and near-infrared spectra were recorded with a Perkin-Elmer Model 300 spectrophotometer. Fourier transform infrared spectroscopy on KBr pellets was performed on IBM IR/32 and Mattson Cygnus 400 instruments. Raman spectra of 1–10 mM $CH_2Cl_2$ solutions were obtained by using argon and krypton ion lasers (Coherent Radiation 52, Spectra Physics 164, and Innova 70), as described previously.[30]

Cyclic voltammetry experiments were performed with a Princeton Applied Research Model 173 potentiostat and Model 175 universal programmer and recorded on a Houston Instruments Model 2000 X-Y recorder. The supporting electrolyte was 0.1 M tetra-*n*-butylammonium perchlorate in $CH_2Cl_2$ or 0.1 M $LiClO_4$ in $CH_3CN$. A Pt disk working electrode, a Pt wire auxiliary electrode, and a Ag/AgCl reference electrode fitted with a vycor plug at the solution junction were employed.

**Preparation of Compounds. ($\mu$-Hydroxo)bis($\mu$-acetato)bis(hydrotris(1-pyrazolyl)borato)diiron(III) Perchlorate, $[Fe_2(OH)(O_2CCH_3)_2(HBpz_3)_2](ClO_4)$ (1).** A solution of 0.50 g (1.98 mmol) of $KHBpz_3$ in 20 mL of water was added to a stirred mixture of 2.12 g (3.97 mmol) of $Fe(ClO_4)_3\cdot 10H_2O$ and 1.08 g (7.94 mmol) of $NaO_2CCH_3\cdot 3H_2O$ in 20 mL of water, causing immediate precipitation of a golden brown solid. After the suspension was stirred for several minutes, the precipitate was removed by filtration, dried briefly in air, and dissolved in 50 mL of $CH_2Cl_2$. Water was removed from the organic phase by using $Na_2SO_4$, whereupon the solution was evaporated to dryness. The residue was dissolved in 50 mL of $CH_2Cl_2$, and 50 mL of diethyl ether was layered on top, causing orange-brown crystals to form after several days. These crystals were collected by filtration and washed with 4 × 1 mL of $CH_2Cl_2$, which removes traces of $[Fe(HBpz_3)_2]^+$ salts, and then by 5 mL of $CH_2Cl_2$/diethyl ether (1:2) to yield 0.19 g (23% based on $KHBpz_3$) of $1\cdot CH_2Cl_2$.

**Caution:** *Perchlorate salts of compounds containing organic ligands are potentially explosive!*[33]

A higher yield of **1** was obtained by adding 5 mL of a 0.25 M (1.25 mmol) solution of $HClO_4$ in diethyl ether, prepared by suspending 0.72 g of 70% aqueous $HClO_4$ in 30 mL of diethyl ether and drying over $Na_2SO_4$, to a solution containing 0.192 g (0.230 mmol) of $[Fe_2O(O_2CCH_3)_2(HBpz_3)_2]\cdot 4CH_3CN$ (**5**) in 70 mL of diethyl ether with rapid stirring. A finely divided yellow-orange precipitate, which immediately formed, was removed by filtration and washed well with diethyl ether to remove any excess acid. The orange solid was dissolved in 100 mL of $CH_2Cl_2$ and purified by vapor diffusion of diethyl ether into the solution at 5 °C, which effected crystallization of 0.127 g (0.148 mmol, 65%) of $1\cdot CH_2Cl_2\cdot H_2O$. After being powdered and dried under vacuum, the compound analyzed for $1\cdot H_2O$. Anal. Calcd for $C_{22.5}H_{28}B_2Cl_2Fe_2N_{12}O_8$ ($1\cdot 0.5CH_2Cl_2$, first method): C, 33.17; H, 3.46; Cl, 8.70; N, 20.63. Found: C, 32.81; H, 3.63; Cl, 8.68; N, 20.38. Calcd for $C_{22}H_{29}B_2ClFe_2N_{12}O_9$ ($1\cdot H_2O$, second method): C, 33.43; H, 3.70; Cl, 4.49; N, 21.27. Found: C, 33.44; H, 3.60; Cl, 4.60; N, 21.17. $^1H$ NMR ($CD_2Cl_2$): $\delta$ 69 ppm (br), 61 (br), 37 (br), 28 (br), −14 (br). EPR (solid, 78 K, 9.165 GHz): 0.5 kOe, 1.23, 2.00, 2.85, 4.4, 5.5 (see Figure S1, supplementary material). UV–vis–near-IR ($CH_2Cl_2$): $\lambda$ 260 nm (sh, $\epsilon_{Fe}$ 5800 $cm^{-1}$ $M^{-1}$), 375 (4750), ~1115 (~0.9). IR (KBr): 3641 $cm^{-1}$, 3566 (OH), 3129, 2511 (BH), 1566 ($\nu_s$, COO), 1505, 1442 ($\nu_{as}$, COO), 1389, 1310, 1212, 1115 ($ClO_4$), 1075, 1051, 985, 873, 814, 769, 715, 659, 624 ($ClO_4$), 559, 500. Raman (488 nm, $CH_3CN$; 455, 488 nm, $CH_2Cl_2$): 925 $cm^{-1}$ ($ClO_4$), 660, 355, 170. FAB-MS (*m/e*): 673 ($M^+$, 9%), 613 ($M-O_2CCH_3$ + H, 76), 554 ($M-2O_2CCH_3$ + H, 18).

**($\mu$-Hydroxo)bis($\mu$-diphenyl phosphato)bis(hydrotris(1-pyrazolyl)borato)diiron(III) Tetrafluoroborate, $[Fe_2(OH)\{O_2P(OC_6H_5)_2\}_2(HBpz_3)_2](BF_4)$ (2).** A solution of 0.5 M $HBF_4\cdot Et_2O$ in diethyl ether (~1 mL, 0.5 mmol) was added under rapid stirring to a solution of 0.537 g (0.445 mmol) of $[Fe_2O\{O_2P(OC_6H_5)_2\}_2(HBpz_3)_2]\cdot CCl_4$ in 130 mL of diethyl ether until no more precipitation of yellow-orange solid was observed and the green color had disappeared. The mixture was filtered, and the precipitate was washed generously with diethyl ether. After drying in air, the product was dissolved in 15 mL of $CH_2Cl_2$, and the solution was stored at 5 °C, allowing ether vapor to diffuse into it. After 3 days, orange crystals of $2\cdot CH_2Cl_2\cdot 0.5Et_2O\cdot H_2O$ (0.38 g, 0.29 mmol, 65%) had appeared and were found to be suitable for X-ray crystallography. The crystals were powdered and dried in air. Anal. Calcd for

(23) Murch, B. P.; Bradley, F. L.; Boyle, P. D.; Papaefthymiou, V.; Que, L., Jr. *J. Am. Chem. Soc.* **1987**, *109*, 7993–8003.
(24) Murch, B. P.; Boyle, P. D.; Que, L., Jr. *J. Am. Chem. Soc.* **1985**, *107*, 6728–6729.
(25) Chiari, B.; Piovesana, O.; Tarantelli, T.; Zanazzi, P. F. *Inorg. Chem.* **1983**, *22*, 2781–2784.
(26) Bailey, N. A.; McKenzie, E. D.; Worthington, J. M.; McPartlin, M.; Tasker, P. A. *Inorg. Chim. Acta* **1977**, *25*, L137.
(27) Hotzelmann, R.; Wieghardt, K.; Ensling, J.; Romstedt, H.; Gütlich, P.; Bill, E.; Flörke, U.; Haupt, H.-J. *J. Am. Chem. Soc.* **1992**, *114*, 9470–9483.
(28) Armstrong, W. H.; Lippard, S. J. *J. Am. Chem. Soc.* **1984**, *106*, 4632–4633.
(29) Scheidt, W. R.; Cheng, B.; Safo, M. K.; Cukiernik, F.; Marchon, J.-C.; Debrunner, P. G. *J. Am. Chem. Soc.* **1992**, *114*, 4420–4421.
(30) Armstrong, W. H.; Spool, A.; Papaefthymiou, G. C.; Frankel, R. B.; Lippard, S. J. *J. Am. Chem. Soc.* **1984**, *106*, 3653–3667.
(31) Turowski, P. N.; Armstrong, W. H.; Roth, M. E.; Lippard, S. J. *J. Am. Chem. Soc.* **1990**, *112*, 681–690.
(32) Armstrong, W. H.; Lippard, S. J. *J. Am. Chem. Soc.* **1985**, *107*, 3730–3731.
(33) Wolsey, W. C. *J. Chem. Educ.* **1973**, *50*, A335–A337.

**Table 1.** Summary of Crystal Data, Intensity Collection, and Structure Refinement Parameters for $[Fe_2(OH)(O_2CCH_3)_2(HBpz_3)_2](ClO_4)\cdot CH_2Cl_2$ (**1**), $[Fe_2(OH)\{O_2P(OC_6H_5)_2\}_2(HBpz_3)_2](BF_4)\cdot 2CH_2Cl_2\cdot 0.5(CH_3CH_2)_2O\cdot H_2O$ (**2**), $[Fe_2(OH)\{O_2P(C_6H_5)_2\}_2(HBpz_3)_2](BF_4)\cdot 2.5(CH_3)_2CO$ (**3**), and $[Fe_2\{O_2P(OC_6H_5)_2\}_3(HBpz_3)_2](BF_4)\cdot CH_2Cl_2$ (**4**)[a]

| formula | $C_{23}H_{29}B_2Cl_3Fe_2N_{12}O_9$ | $C_{46}H_{52}B_3Cl_4F_4Fe_2N_{12}O_{10.5}P_2$ | $C_{49.5}H_{56}B_3F_4Fe_2N_{12}O_{7.5}P_2$ | $C_{55}H_{52}B_3Cl_2F_4Fe_2N_{12}O_{12}P_3$ |
|---|---|---|---|---|
| fw | 857.23 | 1364.87 | 1221.13 | 1457.03 |
| space group | $P2_1/n$ (No. 14) | $C2/c$ (No. 15) | $C2/m$ (No. 12) | $P\bar{1}$ (No. 2) |
| $a$, Å | 11.757(2) | 21.156(4) | 16.772(2) | 12.346(2) |
| $b$, Å | 19.925(4) | 20.518(2) | 33.585(4) | 15.084(2) |
| $c$, Å | 15.580(2) | 27.157(4) | 10.9019(9) | 17.633(2) |
| $\alpha$, deg | | | | 97.50(1) |
| $\beta$, deg | 92.03(1) | 104.268(7) | 105.206(8) | 99.02(1) |
| $\gamma$, deg | | | | 95.76(1) |
| $V$, Å$^3$ | 3647(2) | 11425(3) | 5926(2) | 3191(2) |
| $T$, °C | −15 | −38 | −54 | −54 |
| $Z$ | 4 | 8 | 4 | 2 |
| $D_{calcd}$, g cm$^{-1}$ | 1.561 | 1.587 | 1.369 | 1.516 |
| $D_{obsd}$,[b] g cm$^{-1}$ | 1.55(1) | 1.48(1) | 1.40(1) | 1.48(1) |
| abs coeff, cm$^{-1}$ | 10.76 | 7.82 | 6.10 | 6.90 |
| data collcd | $3° \le 2\theta \le 48°$ $\pm h,+k,+l$ | $3° \le 2\theta \le 48°$ $\pm h,+k,+l$ | $3° \le 2\theta \le 55°$ $\pm h,+k,+l$ | $3° \le 2\theta \le 50°$ $\pm h,\pm k,+l$ |
| no. of data collcd | 6500 | 9689 | 7264 | 11 596 |
| no. of unique data | 5896 | 6088 | 6907 | 11 198 |
| no. of unique data ($I > 3\sigma(I)$) | 3631 | 5883 | 4776 | 8583 |
| no. of variable params | 318 | 731 | 369 | 865 |
| $R_1$[c] | 0.048 | 0.069 | 0.055 | 0.044 |
| $R_2$[c] | 0.052 | 0.078 | 0.070 | 0.062 |
| max peak, e/Å$^3$ | 1.09 | 1.51 | 1.75 | 1.03 |
| min peak, e/Å$^3$ | −0.99 | −1.11 | −0.83 | −1.07 |

[a] Using Mo K$\alpha$ radiation (0.710 69 Å). [b] By suspension in a mixture of $CCl_4$ and toluene at 25 °C. [c] $R_1 = \sum||F_o| - |F_c||/\sum|F_o|$; $R_2 = [\sum w(|F_o| - |F_c|)^2/\sum wF_o^2]^{1/2}$, where $w = 1/\sigma^2(F_o^2)$.

$C_{42}H_{41}B_3F_4Fe_2N_{12}O_9P_2$: C, 44.25; H, 3.63; N, 14.74. Found: C, 44.08; H, 3.87; N, 14.72. $^1$H NMR ($CD_2Cl_2$): $\delta$ 62 ppm (br), 37 (br), 29 (br), 8.25, 8.05, 7.2, 7.1, 1.7 (br), −14 (br). EPR (4 K): 1.65 kOe, 1.88, 2.15, 4.2, >15 (see Figure S1). UV–vis–near-IR ($CH_2Cl_2$): $\lambda$ 260 nm (sh, $\epsilon_{Fe}$ 5800 cm$^{-1}$ M$^{-1}$), 372 (4300), ~1020 (~0.6). IR (KBr): $\nu$ 3130 cm$^{-1}$, 2525 (B–H), 1610, 1591, 1504, 1490, 1404, 1388, 1310, 1212, 1195 ($PO_2$ $\nu_{as}$), 1163 (PO–C), 1115, 1084, 1052, 1027 ($PO_2$ $\nu_s$), 1009, 986, 957, 941 (P–OC), 908, 770 ($BF_4$), 757, 713, 690, 663, 659, 613, 534 ($BF_4$), 518. Raman (514.5 nm, $Me_2CO$): 1598 cm$^{-1}$, 1512, 1412, 1392, 1316, 1224, 1192, 1092, 1022, 554. FAB-MS ($m/e$): 1140 ($MBF_4$, 16%), 1072 (M + F, 19), 1054 (M + H, 100), 1037 (M − O, 26), 803 (M − $HO_2P(OC_6H_5)_2$, 9), 787 (M − OH − $O_2P(OC_6H_5)_2$, 35).

**($\mu$-Hydroxo)bis($\mu$-diphenylphosphinato)bis(hydrotris(1-pyrazolyl)borato)diiron(III) Tetrafluoroborate, $[Fe_2(OH)\{O_2P(C_6H_5)_2\}_2(HBpz_3)_2](BF_4)$ (3).** This compound was prepared from $[Fe_2O\{O_2P(C_6H_5)_2\}_2(HBpz_3)_2]\cdot CH_2Cl_2\cdot CCl_4$ (0.30 g, 0.24 mmol) and isolated in a manner analogous to that reported for **2** to yield 0.18 g (0.15 mmol, 61%) of $3\cdot CH_2Cl_2\cdot H_2O$ after crystallization of the yellow precipitate by vapor diffusion of diethyl ether into a $CH_2Cl_2$ solution of the product. These crystals were not of high enough quality for X-ray crystallography and were thus recrystallized by vapor diffusion of petroleum ether into an acetone solution to yield $3\cdot 2.5Me_2CO$. The sample for analysis was crushed and dried in air. Anal. Calcd for $C_{45}H_{47}B_3F_4Fe_2N_{12}O_6P_2$ ($3\cdot Me_2CO$): C, 47.66; H, 4.18; N, 14.82. Found: C, 47.88; H, 4.24; N, 15.09. UV–vis ($CH_3CN$): $\lambda$ 259 nm (sh), 265 (sh), 272 (sh), 346 ($\epsilon_{Fe}$ 3860 cm$^{-1}$ M$^{-1}$). $^1$H NMR: $\delta$ 64 ppm (br), 41 (br), 36 (br), 13.0, 12.0, 6.7, 6.0, 1.7, −14 (br). EPR (4 K): 1.72 kOe, 1.92, 2.15, 2.27, 4.2, 14 (see Figure S1). IR (KBr): 3148 cm$^{-1}$, 3122, 3060, 2522 (BH), 1629, 1593, 1504, 1441, 1404, 1389, 1310, 1213, 1138 ($PO_2$ $\nu_{as}$), 1118, 1099, 1084, 1070 ($BF_4$), 1052, 1038, 1024 ($PO_2$ $\nu_s$), 1016, 995 (P–C), 984, 787, 765, 755, 727, 715, 695, 665, 660, 621, 557, 549, 532 ($BF_4$), 419, 415, 410. Raman (408 nm, $CH_2Cl_2$): 760 cm$^{-1}$, 330, 307, 258. FAB-MS ($m/e$): 1047 (M + $BF_3$, 13%), 995 (M + O, 100), 980 (M + H, 19), 763 (M + H − $O_2P(C_6H_5)_2$, 37).

**Tris($\mu$-diphenyl phosphato)bis(hydrotris(1-pyrazolyl)borato)diiron(III) Tetrafluoroborate, $[Fe_2\{O_2P(OC_6H_5)_2\}_3(HBpz_3)_2](BF_4)$ (4).** A solution of 0.27 g (1.07 mmol) of $HO_2P(OC_6H_5)_2$ in 10 mL of $CH_2Cl_2$ was added dropwise over 5 min to an agitated solution of 0.40 g (0.48 mmol) of $[Fe_2O(O_2CCH_3)_2(HBpz_3)_2]\cdot 4CH_3CN$ in 200 mL of $CH_2Cl_2$. A rapid color change from brown-green to emerald green indicated that the reaction proceeded readily. After 15 min, the solvent was removed with a rotary evaporator and the resulting dark green oil was dissolved in 30 mL of $CCl_4$. The mixture was filtered to remove impurities, and again the solvent was removed with a rotary evaporator. The green residue was dissolved in 50 mL of diethyl ether, and 2.5 mL (0.88 mmol) of a solution of 0.35 M $HBF_4\cdot Et_2O$ in ether was added dropwise with stirring, causing quantitative precipitation of a yellow-orange solid. The mixture was filtered, and the precipitate was washed generously with ether. After drying in air, the product was dissolved in 5 mL of $CH_2Cl_2$, and the solution was stored at 5 °C, allowing ether vapor to diffuse into it. After 3 days, 0.47 g (0.32 mmol, 89%) of large red-orange needles of $4\cdot CH_2Cl_2$ was obtained and found to be suitable for X-ray crystallography. The crystals were powdered and dried in air prior to elemental analysis and further characterization. Anal. Calcd for $C_{54}H_{50}B_3F_4Fe_2N_{12}O_{12}P_3$: C, 47.27; H, 3.67; N, 12.25. Found: C, 47.09; H, 3.69; N, 12.18. $^1$H NMR: $\delta$ 100 ppm (br), 50 (br), 32 (br), 8.4, 6.8, −14 (br). UV–vis ($Et_2O$): $\lambda$ 248 nm (sh), 255 (sh), 261 (sh), 267 (sh), 376 ($\epsilon_{Fe}$ ~5000 cm$^{-1}$ M$^{-1}$). IR (KBr): $\nu$ 3220 cm$^{-1}$, 3150, 2522 (B–H), 1592, 1505, 1491, 1405, 1390, 1311, 1213, 1196 ($PO_2$ $\nu_{as}$), 1164 (PO–C), 1115, 1084, 1053, 1029 ($PO_2$ $\nu_s$), 1010, 987, 957, 942 (P–OC), 780, 765, 714, 691, 664, 660, 619, 534 ($BF_4$), 519.

**X-ray Crystallography.** An orange-brown rectangular prism of $1\cdot CH_2Cl_2$ was flame-sealed in a glass capillary to prevent solvent loss from the lattice. Study on the diffractometer revealed that it crystallizes in the monoclinic system. A golden orange block-shaped monoclinic crystal of $2\cdot 2CH_2Cl_2\cdot 0.5Et_2O\cdot H_2O$, a golden yellow block-shaped monoclinic crystal of $3\cdot 2.5Me_2CO$, and an orange-red elongated triclinic crystal of $4\cdot CH_2Cl_2$ were selected and mounted with epoxy resin on thin glass fibers under a cold stream of $N_2$. Relevant crystallographic information for the complexes is presented in Table 1. Unit cell parameters and intensity data were obtained by using the general procedures previously described.[34] Corrections were applied for Lorentz and polarization effects in all data sets and for 1.8% crystal decay in the case of $3\cdot 2.5Me_2CO$. Empirical absorption corrections were applied to the data of $2\cdot 2CH_2Cl_2\cdot 0.5Et_2O\cdot H_2O$ and $4\cdot CH_2Cl_2$, and an analytical correction was used for $3\cdot 2.5Me_2CO$. The structures were solved by using the direct methods program MULTAN and standard difference Fourier methods in the TEXSAN, SHELXS, and SHELX packages.[35-38] The positions of all non-hydrogen atoms were refined with anisotropic thermal parameters, except for the ether and one of the $CH_2Cl_2$ molecules in $2\cdot 2CH_2Cl_2\cdot 0.5Et_2O\cdot H_2O$, which were refined isotropically, and the $BF_4^-$ anions in $3\cdot 2.5Me_2CO$, which

(34) Carnahan, E. M.; Rardin, R. L.; Bott, S. G.; Lippard, S. J. *Inorg. Chem.* **1992**, *31*, 5193–5201.
(35) *International Tables for X-ray Crystallography*, 3rd ed.; Kynoch Press: Birmingham, England, 1973; Vol. IV.
(36) *TEXSAN: Single Crystal Structure Analysis Software, Version 5.0*; Molecular Structure Corporation: The Woodlands, TX, 1989.
(37) Sheldrick, G. M. In *Crystallography Computing*; Sheldrick, G. M., Krüger, C., Goddard, R., Eds.; Oxford University Press: Oxford, U.K., 1985; pp 175–189.
(38) Sheldrick, G. M. In *Computing in Crystallography*; Schenk, H., Olthof-Hagenkamp, R., van Koningsveld, H., Bassi, G. C., Eds.: Delft University Press: Delft, The Netherlands, 1978; pp 34–42.

**Table 2.** Atomic Coordinates for Coordination Spheres in Compounds **1–4**

| atom | x | y | z |
|---|---|---|---|
| | $[Fe_2(OH)(O_2CCH_3)_2(HBpz_3)_2](ClO_4)\cdot CH_2Cl_2$ (**1**) | | |
| Fe1 | 0.14663(6) | 0.11949(4) | 0.83642(5) |
| Fe2 | 0.36815(6) | 0.01258(4) | 0.79663(5) |
| O | 0.2351(3) | 0.0647(2) | 0.7584(2) |
| H | 0.2058 | 0.0687 | 0.7139 |
| O11 | 0.1481(3) | 0.0461(2) | 0.9237(2) |
| O12 | 0.2863(3) | 0.1604(2) | 0.8916(3) |
| O21 | 0.2859(3) | −0.0272(2) | 0.8949(3) |
| O22 | 0.4271(3) | 0.0869(2) | 0.8720(3) |
| N11 | −0.0087(4) | 0.3243(2) | 0.2418(3) |
| N12 | 0.0431(4) | 0.1806(2) | 0.9121(3) |
| N13 | 0.1341(4) | 0.1971(2) | 0.7464(3) |
| N21 | 0.3218(4) | −0.0676(2) | 0.7159(3) |
| N22 | 0.5149(4) | −0.0440(2) | 0.8274(3) |
| N23 | 0.4659(4) | 0.0480(2) | 0.6952(3) |
| | $[Fe_2(OH)\{O_2P(OC_6H_5)_2\}_2(HBpz_3)_2](BF_4)\cdot 2CH_2Cl_2\cdot 0.5(CH_3CH_2)_2O\cdot H_2O$ (**2**) | | |
| Fe1 | 0.40551(4) | 0.16392(4) | 0.38803(3) |
| Fe2 | 0.55444(4) | 0.25530(4) | 0.42185(4) |
| O | 0.4748(2) | 0.2199(2) | 0.3753(2) |
| H | 0.467(3) | 0.231(3) | 0.351(2) |
| P1 | 0.53530(9) | 0.11352(9) | 0.46784(7) |
| P2 | 0.43556(8) | 0.27796(8) | 0.47338(7) |
| O11 | 0.4713(2) | 0.1044(2) | 0.4314(2) |
| O12 | 0.3997(2) | 0.2209(2) | 0.4461(2) |
| O21 | 0.5743(2) | 0.1696(2) | 0.4580(2) |
| O22 | 0.5056(2) | 0.2866(2) | 0.4716(2) |
| N11 | 0.3998(3) | 0.1025(3) | 0.3256(2) |
| N12 | 0.3323(3) | 0.1020(3) | 0.4041(2) |
| N13 | 0.3279(3) | 0.2137(3) | 0.3390(2) |
| N21 | 0.6113(3) | 0.2284(3) | 0.3707(2) |
| N22 | 0.6418(2) | 0.2957(3) | 0.4664(2) |
| N23 | 0.5436(3) | 0.3457(3) | 0.3851(2) |
| | $[Fe_2(OH)\{O_2P(C_6H_5)_2\}_2(HBpz_3)_2](BF_4)\cdot 2.5(CH_3)_2CO$ (**3**) | | |
| Fe1 | 0.09600(3) | 0.34964(1) | 0.11840(5) |
| O | 0.0000 | 0.3749(1) | 0.0000 |
| H | 0.0000 | 0.3922 | 0.0000 |
| O11 | 0.0257(1) | 0.31745(8) | 0.2009(2) |
| O12 | 0.0979(1) | 0.30659(7) | −0.0046(2) |
| P1 | −0.05673(5) | 0.29724(3) | 0.14257(9) |
| N11 | 0.2027(2) | 0.3243(1) | 0.2418(3) |
| N12 | 0.1088(2) | 0.3931(1) | 0.2621(3) |
| N13 | 0.1813(2) | 0.3860(1) | 0.0548(3) |
| | $[Fe_2\{O_2P(OC_6H_5)_2\}_3(HBpz_3)_2](BF_4)\cdot CH_2Cl_2$ (**4**) | | |
| Fe1 | 0.39638(4) | 0.59762(3) | 0.20683(3) |
| Fe2 | 0.28781(4) | 0.88676(3) | 0.23266(3) |
| P1 | 0.41731(7) | 0.75210(6) | 0.35336(5) |
| P2 | 0.47301(7) | 0.79548(5) | 0.14614(5) |
| P3 | 0.15393(7) | 0.68180(6) | 0.18495(5) |
| O11 | 0.3974(2) | 0.6564(1) | 0.3135(1) |
| O12 | 0.4711(2) | 0.7113(1) | 0.1824(1) |
| O13 | 0.1811(2) | 0.6240(2) | 0.1745(1) |
| O21 | 0.3688(2) | 0.8221(1) | 0.3116(1) |
| O22 | 0.3826(2) | 0.8525(2) | 0.1546(1) |
| O23 | 0.1811(2) | 0.7802(1) | 0.1846(1) |
| N11 | 0.3448(2) | 0.4723(2) | 0.2383(2) |
| N12 | 0.5529(2) | 0.5538(2) | 0.2279(2) |
| N13 | 0.3822(2) | 0.5285(2) | 0.0940(2) |
| N21 | 0.1787(2) | 0.9287(2) | 0.3061(2) |
| N22 | 0.3884(2) | 1.0054(2) | 0.2817(2) |
| N23 | 0.2113(2) | 0.9677(2) | 0.1564(2) |

were refined as rigid groups. Partial disorder, which occurred at some of the solvent molecules and anions, was accounted for in the models. The H atoms were placed at calculated positions for the final refinement cycles (C–H = 0.95 Å), except for the O–H hydrogens in **1–3**, which were located from the difference Fourier maps. Further details are given elsewhere.[34] Final refinement parameters, selected positional parameters, and selected bond distances and angles are provided in Tables 1–3, respectively. Listings of final positional parameters for all atoms may be found in the supplementary material as Tables S1–S4, thermal parameters for non-hydrogen atoms are supplied in Tables S5–S8, and full lists of bond distances and angles are given in Tables S9–S12.

**Magnetic Susceptibility Measurements.** The solution magnetic susceptibilities of **1** and **2**, in $CD_2Cl_2$, and of **3** and **4**, in $CDCl_3$, were measured by the Evans NMR technique.[39,40] Diamagnetic corrections of −346.7 × $10^{-6}$ cgs mol$^{-1}$ for **1**·0.5$CH_2Cl_2$, −577.4 × $10^{-6}$ cgs mol$^{-1}$ for **2**, −580.9 × $10^{-6}$ cgs mol$^{-1}$ for **3**·$H_2O$·0.2$CH_2Cl_2$, and −712.7 × $10^{-6}$ cgs mol$^{-1}$ for **4** were calculated from Pascal's constants.[41–43] Solid-state measurements of 17.41 mg of powdered **1**·0.5$CH_2Cl_2$, in an Al–Si sample container, and of 103.6 mg of powdered **2**, 39.4 mg of powdered **3**·$H_2O$·0.2$CH_2Cl_2$, and 24.0 mg of powdered **4**, in polyethylene sample containers, were carried out at the Francis Bitter National Magnet Laboratory with an SHE Model 905 SQUID susceptometer operated at 10 kG. All samples were recrystallized at least twice. A total of 66 data points were obtained over the range 4–300 K for **1**, and 45–46 data points over 6–300 K for **2–4**. The moment of the sample holders was measured at the same temperature points and subtracted from the observed moment with sample present. The field dependence of the magnetic susceptibility of **1** and **2** was investigated at various temperatures.

## Results and Discussion

**Syntheses.** The hydroxo-bridged dinuclear complex $[Fe_2(OH)(O_2CCH_3)_2(HBpz_3)_2](ClO_4)$, **1**, was prepared in two different ways. It could be isolated from a mixture of ferric ion, acetate, and hydrotris(1-pyrazolyl)borate in water or by protonation of the $\mu$-oxo complex $[Fe_2O(O_2CCH_3)_2(HBpz_3)_2]$, **5**. The former synthesis afforded a lower yield of **1**, requiring isolation from mixtures containing larger amounts of **5** and of $[Fe(HBpz_3)_2]^+$. The protonation reaction provided higher yields (59–65%) and could be applied to the synthesis of other hydroxo-bridged complexes, $[Fe_2(OH)\{O_2P(OC_6H_5)_2\}_2(HBpz_3)_2](BF_4)$ (**2**) and $[Fe_2(OH)\{O_2P(C_6H_5)_2\}_2(HBpz_3)_2](BF_4)$ (**3**), as described in eq 1. Side products of the reaction are the $[Fe(HBpz_3)_2]^+$

$$[Fe_2O(O_2R)_2(HBpz_3)_2] \underset{Et_3N}{\overset{HX}{\rightleftharpoons}} [Fe_2(OH)(O_2R)_2(HBpz_3)_2](X) \quad (1)$$

$$R = CCH_3,\ P(OC_6H_5)_2,\ P(C_6H_5)_2;\ X = ClO_4^-,\ BF_4^-$$

cation and polymeric iron phosphate materials. When a base such as triethylamine was added to a solution containing **1**, the optical spectrum of the oxo-bridged complex **5** was regenerated, demonstrating that the protonation reaction is reversible. Since **1** and **5** are present in approximately equal amounts in aqueous solutions of ferric perchlorate, sodium acetate, and $KHBpz_3$ at pH 3.5,[28,30] we estimate the p$K_a$ to be ~3.5 for deprotonation of the hydroxo bridge. This value is similar to that reported for $[L'Ru(OH)(O_2CCH_3)_2FeL]^{3+}$, where L is 1,4,7-triazacyclononane and L' is 1,4,7-trimethyl-1,4,7-triazacyclononane.[27]

In the presence of excess diphenyl phosphate, it was also possible to obtain the tris(phosphate)-bridged complex $[Fe_2\{O_2P(OC_6H_5)_2\}_3(HBpz_3)_2](BF_4)$, **4**, under the acidic conditions given in eq 1. Similar compounds, $[Fe_2(O_3POC_6H_5)_3(metacn)_2]$ and $[Fe_2(HPO_4)_3(metacn)_2]$, where metacn is 1,4,7-trimethyl-1,4,7-triazacyclononane, have been reported but not structurally characterized; crystal structures of tris(arsenate)- and tris(chromate)-bridged analogues have been obtained.[44,45] Oxo-bridged bis(phosphate)-bridged compounds have appeared in the literature, as have the tris(phosphate)-bridged molecules described above.[13,31,44,45] Aryloxide- and alkoxide-bridged diiron(III) complexes with bridging or terminal phosphates have been

(39) Evans, D. F. *J. Chem. Soc.* **1958**, 2003–2005.
(40) Live, D. H.; Chan, S. I. *Anal. Chem.* **1970**, *42*, 791–792.
(41) Carlin, R. L. *Magnetochemistry*; Springer-Verlag: New York, 1986; pp 3–33.
(42) O'Connor, C. J. *Prog. Inorg. Chem.* **1982**, *29*, 203–283.
(43) Karlin, K. D. Ph.D. Dissertation, Columbia University, 1975.
(44) Drüecke, S.; Wieghardt, K.; Nuber, B.; Weiss, J.; Fleischhauer, H.-P.; Gehring, S.; Haase, W. *J. Am. Chem. Soc.* **1989**, *111*, 8622–8631.
(45) Chaudhuri, P.; Winter, M.; Wieghardt, K.; Gehring, S.; Haase, W.; Nuber, B.; Weiss, J.; *Inorg. Chem.* **1988**, *27*, 1564–1569.

**Table 3.** Selected Interatomic Distances (Å) and Angles (deg) for $[Fe_2(OH)(O_2CCH_3)_2(HBpz_3)_2](ClO_4)\cdot CH_2Cl_2$ (**1**), $[Fe_2(OH)\{O_2P(OC_6H_5)_2\}_2(HBpz_3)_2](BF_4)\cdot 2CH_2Cl_2\cdot 0.5(CH_3CH_2)_2O\cdot H_2O$ (**2**), $[Fe_2(OH)\{O_2P(C_6H_5)_2\}_2(HBpz_3)_2](BF_4)\cdot 2.5(CH_3)_2CO$ (**3**), and $[Fe_2\{O_2P(OC_6H_5)_2\}_3(HBpz_3)_2](BF_4)\cdot CH_2Cl_2$ (**4**)[a]

| | 1 | 2 | 3 | 4 |
|---|---|---|---|---|
| Fe1–O, Fe2–O | 1.959(4), 1.953(4) | 1.960(5), 1.979(4) | 1.972(2) | |
| Fe1–O11, Fe1–O12 | 1.996(4), 2.000(4) | 2.001(4), 1.990(5) | 1.978(3), 1.981(3) | 1.970(2), 1.994(2) |
| Fe2–O21, Fe2–O22 | 2.003(4), 1.999(4) | 2.008(4), 1.997(5) | | 2.001(2), 1.994(2) |
| Fe1–O13, Fe2–O23 | | | | 1.983(2), 1.976(2) |
| Fe1–N11, Fe1–N13 | 2.105(5), 2.090(5) | 2.093(6), 2.106(5) | 2.115(3), 2.131(4) | 2.105(3), 2.095(3) |
| Fe2–N21, Fe2–N23 | 2.094(5), 2.108(5) | 2.123(6), 2.091(5) | | 2.097(3), 2.110(3) |
| Fe1–N12, Fe2–N22 | 2.111(5), 2.103(5) | 2.129(6), 2.112(5) | 2.112(3) | 2.098(3), 2.076(3) |
| Fe1···P1, Fe1···P2 | | 3.221(2), 3.244(2) | 3.175(1), 3.262(1) | 3.205(1), 3.396(1) |
| Fe2···P1, Fe2···P2 | | 3.230(2), 3.199(2) | | 3.453(1), 3.260(1) |
| Fe1···P3, Fe2···P3 | | | | 3.354(1), 3.295(1) |
| Fe1···Fe2 (Fe1···Fe1′) | 3.439(1) | 3.586(1) | 3.5599(9) | 4.6771(9) |
| Fe–O–Fe | 123.0(2) | 131.1(3) | 129.1(2) | |
| Fe–O–P (Fe–O–C) | 132.9(4)–136.8(4) | 131.4(3)–137.1(3) | 129.7(2)–137.8(2) | 134.5(1)–164.0(1) |
| FeO–P–OFe (O–C–O) | 117.1(5), 124.8(5) | 116.0(3), 117.4(3) | 116.7(2) | 117.1(1)–118.3(1) |
| O–Fe1–O11 (O13–Fe1–O11) | 91.3(2) | 91.1(2) | 92.92(8) | 90.7(1) |
| O–Fe1–O12 (O13–Fe1–O12) | 92.7(2) | 89.5(2) | 91.5(1) | 96.1(1) |
| O–Fe2–O21 (O23–Fe2–O21) | 92.3(2) | 92.0(2) | | 94.2(1) |
| O–Fe2–O22 (O23–Fe2–O22) | 92.4(2) | 92.8(2) | | 88.5(1) |
| O–Fe1–N11 (O13–Fe1–N11) | 92.2(2) | 96.0(2) | 177.2(1) | 93.6(1) |
| O–Fe1–N12 (O13–Fe1–N12) | 175.5(2) | 178.1(2) | 95.4(1) | 171.7(1) |
| O–Fe1–N13 (O13–Fe1–N13) | 91.3(2) | 96.1(2) | 92.5(1) | 86.1(1) |
| O–Fe2–N21 (O23–Fe2–N21) | 92.0(2) | 91.0(2) | | 90.6(1) |
| O–Fe2–N22 (O23–Fe2–N22) | 175.4(2) | 175.4(2) | | 174.0(1) |
| O–Fe2–N23 (O23–Fe2–N23) | 92.6(2) | 92.6(2) | | 91.6(1) |
| O11–Fe1–O12, O21–Fe2–O22 | 91.1(2), 90.6(2) | 93.5(2), 91.8(2) | 91.5(1) | 90.08(9), 92.81(9) |
| O11–Fe1–N11, O11–Fe1–N12 | 90.4(2), 91.9(2) | 90.1(2), 87.1(2) | 89.8(1), 89.9(1) | 89.9(1), 96.8(1) |
| O12–Fe1–N12, O12–Fe1–N13 | 90.3(2), 91.4(2) | 89.9(2), 91.5(2) | 172.9(1), 93.8(1) | 87.6(1), 94.1(1) |
| O21–Fe2–N21, O21–Fe2–N22 | 92.0(2), 91.6(2) | 90.5(2), 90.9(2) | | 92.9(1), 89.7(1) |
| O22–Fe2–N22, O22–Fe2–N23 | 89.9(2), 90.3(2) | 90.7(2), 91.3(2) | | 94.4(1), 88.7(1) |
| O11–Fe1–N13, O12–Fe1–N11 | 176.3(2), 174.9(2) | 171.3(2), 173.3(2) | 172.3(1), 88.6(1) | 175.0(1), 170.3(1) |
| O21–Fe2–N23, O22–Fe2–N21 | 175.0(2), 174.8(2) | 174.3(2), 175.5(2) | | 174.0(1), 174.3(1) |
| N11–Fe1–N12, N21–Fe2–N22 | 84.7(2), 85.5(2) | 84.7(2), 85.4(2) | 84.4(1) | 82.8(1), 86.1(1) |
| N11–Fe1–N13, N21–Fe2–N23 | 85.4(2), 86.7(2) | 84.2(2), 86.1(2) | 84.8(1) | 86.4(1), 85.6(1) |
| N12–Fe1–N13, N22–Fe2–N23 | 85.4(2), 83.4(2) | 85.7(2), 84.4(2) | 84.2(1) | 86.1(1), 84.3(1) |

| | 1<br>min, max, mean | 2<br>min, max, mean | 3<br>min, max, mean | 4<br>min, max, mean |
|---|---|---|---|---|
| O···$O_{bridge}$ | 2.238(5), 2.240(5), 2.239 | 2.508(6), 2.560(6), 2.534 | 2.585(3) | 2.543(3), 2.562(3), 2.554 |
| P–OFe | | 1.478(5), 1.506(5), 1.488 | 1.514(2), 1.522(3), 1.518 | 1.485(2), 1.499(2), 1.491 |
| P–OC (P–C) | | 1.569(5), 1.589(5), 1.580 | 1.787(4), 1.789(4), 1.788 | 1.566(3), 1.578(2), 1.574 |
| PO–C | | 1.401(8), 1.42(1), 1.41 | | 1.400(4), 1.421(4), 1.411 |
| C–$C_{ph}$ | | 1.31(2), 1.43(2), 1.37 | 1.363(8), 1.399(5), 1.380 | 1.342(5), 1.399(5), 1.375 |
| N–N | 1.357(6), 1.373(6), 1.367 | 1.342(7), 1.382(9), 1.365 | 1.357(4), 1.374(4), 1.365 | 1.365(4), 1.370(4), 1.367 |
| C–N | 1.324(8), 1.353(7), 1.336 | 1.31(1), 1.37(1), 1.34 | 1.329(5), 1.346(6), 1.339 | 1.325(5), 1.342(5), 1.337 |
| B–N | 1.528(8), 1.561(9), 1.544 | 1.52(1), 1.56(1), 1.54 | 1.536(6), 1.538(6), 1.537 | 1.535(5), 1.546(6), 1.539 |
| C–$C_{pyrazole}$ | 1.361(9), 1.392(9), 1.372 | 1.35(1), 1.41(1), 1.38 | 1.362(7), 1.389(7), 1.373 | 1.364(6), 1.385(5), 1.377 |
| B–F (Cl–O) | 1.410(6), 1.424(5), 1.420 | 1.34(1), 1.40(1), 1.37 | 1.360 | 1.24(1), 1.37(1), 1.34 |
| C–Cl | 1.67(1), 1.72(1), 1.70 | 1.67(1), 1.92(4), 1.79 | | 1.77(2), 1.82(2), 1.80 |
| O–C[b] | 1.257(7), 1.270(7), 1.262 | 1.33(4) | 1.19(1), 1.23(2), 1.21 | |
| C–$CH_3$[b] | 1.505(8), 1.508(9), 1.507 | 1.44(4) | 1.45(1), 1.53(1), 1.50 | |

[a] See Figure 1 for labeling schemes. Estimated standard deviations, in parentheses, occur in the last significant figure. Atoms related by the $C_2$ operator are indicated by a prime. [b] For acetate in **1**, ether in **2**, and acetone in **3**.

prepared,[13,46–48] and hydroxo-bridged bis(phosphate)-bridged compounds are presented here.

Cyclic voltammograms of **1**–**3** in different solvents exhibited irreversible reductions accompanied by the appearance of a reversible wave corresponding to $[Fe(HBpz_3)_2]^+$. This behavior is analogous to that of the oxo-bridged analogues of **1**–**3**, despite the difference in charge between the two types of complexes.[28,30,31] The tendency of dinuclear ferric complexes to dissociate upon reduction is significantly diminished in the core environments of diiron proteins which undergo reversible redox reactions, in systems containing specialized dinucleating ligands,[49] and in complexes which cannot decompose to mononuclear ones because of steric hindrance of the ligands.[50] An interesting example of the last case is a heterodinuclear hydroxobis(carboxylato)-bridged $Fe^{III}Ru^{III}$ complex which exhibits a reversible reduction at +0.19 V vs NHE.[27]

**Crystallographic Results.** The structures of $[Fe_2(OH)(O_2CCH_3)_2(HBpz_3)_2](ClO_4)\cdot CH_2Cl_2$ (**1**·$CH_2Cl_2$), $[Fe_2(OH)\{O_2P(OC_6H_5)_2\}_2(HBpz_3)_2](BF_4)\cdot 2CH_2Cl_2\cdot 0.5Et_2O\cdot H_2O$ (**2**·2$CH_2Cl_2$·0.5$Et_2O$·$H_2O$), $[Fe_2(OH)\{O_2P(C_6H_5)_2\}_2(HBpz_3)_2](BF_4)\cdot 2.5Me_2CO$ (**3**·2.5$Me_2CO$), and $[Fe_2\{O_2P(OC_6H_5)_2\}_3(HBpz_3)_2](BF_4)\cdot CH_2Cl_2$ (**4**·$CH_2Cl_2$) are shown in Figure 1, and Table 3 contains selected geometric information for the four complexes. To prevent solvent loss, the structures were obtained at low temperature. Several different crystallization solvents

(46) Jang, H. G.; Hendrich, M. P.; Que, L., Jr. *Inorg. Chem.* **1993**, *32*, 911–918.
(47) Schepers, K.; Bremer, B.; Krebs, B.; Henkel, G.; Althaus, E.; Mosel, B.; Müller-Warmuth, W. *Angew. Chem., Int. Ed. Engl.* **1990**, *29*, 531–533.
(48) Bremer, B.; Schepers, K.; Fleischhauer, P.; Haase, W.; Henkel, G.; Krebs, B. *J. Chem. Soc., Chem. Commun.* **1991**, 510–511.
(49) Watton, S.; Lippard, S. J. Unpublished results.
(50) Hartman, J. R.; Rardin, R. L.; Chaudhuri, P.; Pohl, K.; Wieghardt, K.; Nuber, B.; Weiss, J.; Papaefthymiou, G. C.; Frankel, R. B.; Lippard, S. J. *J. Am. Chem. Soc.* **1987**, *109*, 7387–7396.
(51) Norman, R. E.; Yan, S.; Que, L., Jr.; Backes, G.; Ling, J.; Sanders-Loehr, J.; Zhang, J.; O'Connor, C. J. *J. Am. Chem. Soc.* **1990**, *112*, 1554–1562.

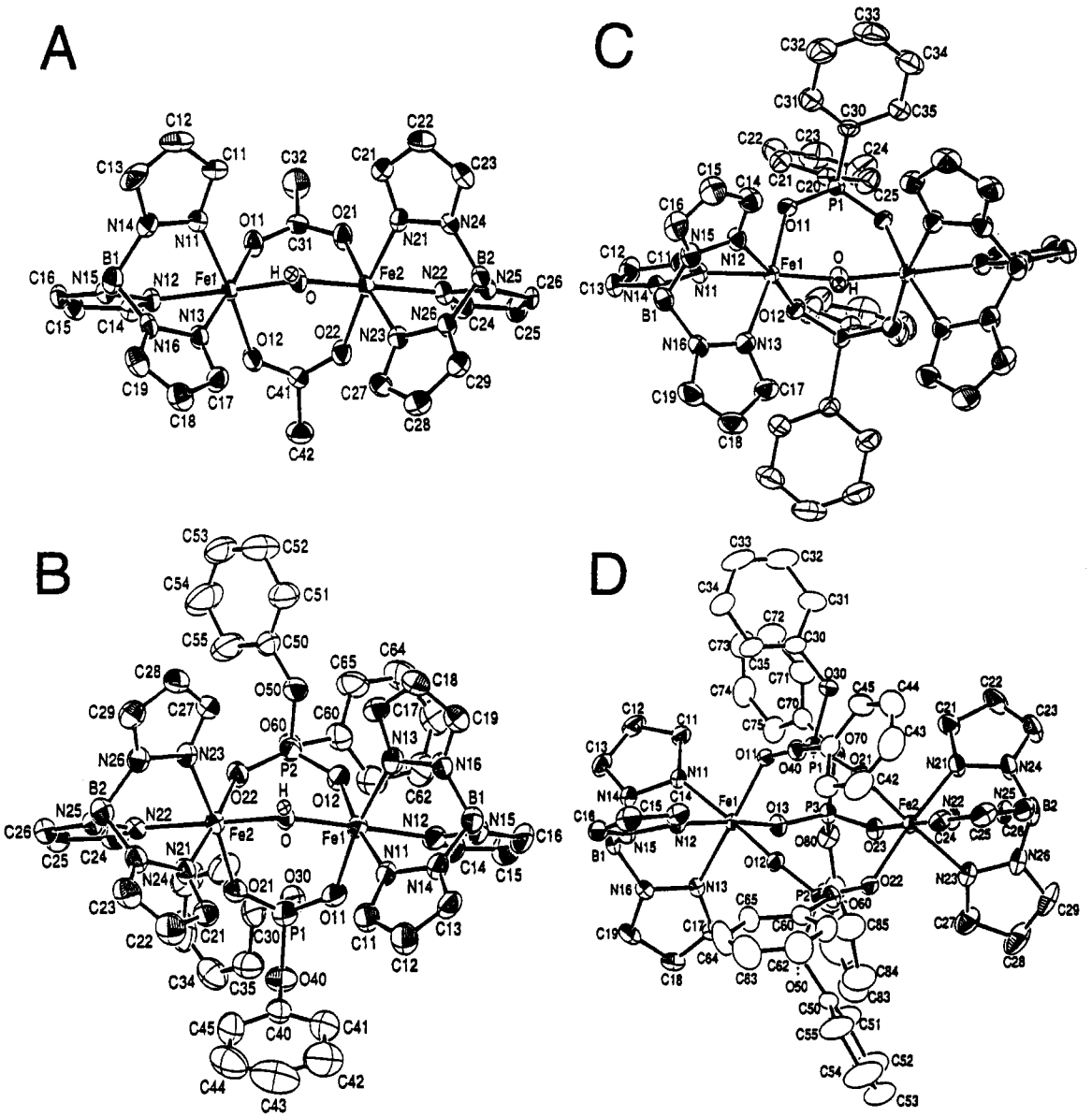


**Figure 1.** Structures of the cations in (A) $[Fe_2(OH)(O_2CCH_3)_2(HBpz_3)_2](ClO_4)\cdot CH_2Cl_2$, (B) $[Fe_2(OH)\{O_2P(OC_6H_5)_2\}_2(HBpz_3)_2](BF_4)\cdot 2CH_2Cl_2\cdot 0.5Et_2O\cdot H_2O$, (C) $[Fe_2(OH)\{O_2P(C_6H_5)_2\}_2(HBpz_3)_2](BF_4)\cdot 2.5Me_2CO$, and (D) $[Fe_2\{O_2P(OC_6H_5)_2\}_3(HBpz_3)_2](BF_4)\cdot CH_2Cl_2$, showing 50% probability thermal ellipsoids and the atom-labeling schemes.

and methods were employed before satisfactory structures for **2** and **3** were obtained, and the arrangement of solvent molecules in the crystal lattice is somewhat unusual for both compounds. The ether molecule in **2** lies on a 2-fold axis, and compound **3** has crystallographically imposed $C_2$ symmetry. One of the acetone molecules in **3** is situated on a mirror plane as well as on a $C_2$ axis; the half acetone molecule, which is disordered about the $C_2$ axis, is similarly placed. Another acetone molecule lies on a mirror plane and is disordered both about the mirror and a $C_2$ axis. Structures **1**–**3** reveal that the ligand-bridged diiron(III) core is retained upon protonation of the oxo bridge in the acetate-, diphenyl phosphate-, and diphenylphosphinate-bridged complexes. The resulting ($\mu$-hydroxo)diiron(III) core is additionally bridged by two bidentate acetate or phosphate ligands, and the $\{Fe_2(OH)(O_2R)_2\}^{2+}$ unit is capped on the two ends by hydrotris(1-pyrazolyl)borate ligands. The iron atoms in the complexes have distorted octahedral geometry, with the largest deviations from the idealized 90° angles occurring in tris(phosphate)-bridged analogue **4** (82.8–96.8°). The octahedral cis angles range from 83.4 to 92.7° in **1**, 84.2 to 96.1° in **2**, and 84.1 to 95.4° in **3**. Some important structural features of **1**–**4** are compared with those of selected compounds in Table 4. The structures of the hydroxo-bridged complexes are similar to one another, and the metal–ligand bond distances are essentially the same in **1**–**3**. Structural differences between phosphate or phosphinate ligands and carboxylate groups result in an expanded core in **2** and **3** relative to **1**, causing larger Fe–OH–Fe angles, 131.2(3) and 129.1(2)° vs 123.0(2)°, and greater Fe···Fe separations, 3.586(1) and 3.560(1) Å vs 3.439(1) Å. As discussed previously, there is an increased O···O bite distance in phosphate or phosphinate compared to carboxylate ligands, caused by longer P–$O_{Fe}$ (~1.49–1.52 Å) than C–$O_{Fe}$ distances (~1.26 Å).[31] The bite distance in carboxylate diiron complexes is around 2.23 Å,[28,30–32,50–56] whereas

(52) Tolman, W. B.; Bino, A.; Lippard, S. J. *J. Am. Chem. Soc.* **1989**, *111*, 8522–8523.
(53) Feng, X.; Bott, S. G.; Lippard, S. J. *J. Am. Chem. Soc.* **1989**, *111*, 8046–8047.
(54) Beer, R. H.; Tolman, W. B.; Bott, S. G.; Lippard, S. J. *Inorg. Chem.* **1989**, *28*, 4557–4559.
(55) Spool, A.; Williams, I. D.; Lippard, S. J. *Inorg. Chem.* **1985**, *24*, 2156–2162.
(56) Armstrong, W. H.; Lippard, S. J. *J. Am. Chem. Soc.* **1983**, *105*, 4837–4838.
(57) Day, R. O.; Chandrasekhar, V.; Kumara Swamy, K. C.; Holmes, J. M.; Burton, S. D.; Holmes, R. R. *Inorg. Chem.* **1988**, *27*, 2887–2893.
(58) Narayanan, P.; Ramirez, F.; McCaffrey, T.; Chaw, Y.; Marecek, J. F. *J. Org. Chem.* **1978**, *43*, 24–31.

**Table 4.** Comparison of Structural, Mössbauer, and Magnetic Parameters of **1–4** to Selected Non-Heme Diiron(III) Complexes and Proteins[a]

| compd | M–O(H) (Å) | M···M (Å) | ∠M–O–M (deg) | M–P (Å) | M–O(C,P) (Å) | O···O (Å) | $\delta$[b] (mm/s) | $\Delta E_Q$[b] (mm/s) | $J$[c] ($cm^{-1}$) |
|---|---|---|---|---|---|---|---|---|---|
| **1** | 1.96 | 3.44 | 123 | | 2.00 | 2.24 | 0.47 | 0.37 | ~–17[m] |
| **2** | 1.97 | 3.59 | 131 | 3.20–3.24 | 2.00 | 2.53 | 0.44 | 0.44 | ~–15 |
| **3** | 1.97 | 3.56 | 129 | 3.18–3.26 | 1.98 | 2.59 | 0.49 | 0.31 | ~–15 |
| **4** | | 4.68 | | 3.20–3.45 | 1.99 | 2.55 | | | –0.8 |
| $[Fe_2O\{O_2P(OC_6H_5)_2\}_2(L)_2]$[d] | 1.81 | 3.34 | 134 | 3.20–3.22 | 2.04 | 2.57 | 0.53 | 1.60 | –97.5 |
| $[Fe_2O(O_2CCH_3)_2(HBpz_3)_2]$[e] | 1.78 | 3.15 | 124 | | 2.04 | 2.24 | 0.52 | 1.60 | –120 |
| $[Fe_3(OH)_2(O_2CPh)_4(N3)_2]^{3+}$[f] | 1.93–1.96 | 3.44 | 124 | | 1.99 | | 0.41 | 0.74 | –17 to –30 |
| $[Fe_3O(O_2CR)_6(H_2O)_3]^+$[g] | 1.90 | 3.30 | 120 | | 2.02 | 2.22 | 0.52 | 0.72–0.93 | –30 |
| $[Fe_2(OH)_2(salam)]$[h] | 1.99–2.06 | 3.12 | 103 | | 2.06 | | 0.49 | 0.56 | –10.4 |
| $[Fe_2(OH)_2(dipic)_2(H_2O)_2]$[i] | 1.94–1.99 | 3.09 | 104 | | 1.99 | | | | –11.4 |
| $Uf_o$-$P_i$[j] | 1.94(2) | 3.27 | 109 | 3.17 | 2.0 | | 0.52, 0.55 | 1.02, 1.38 | <–40 |
| $BPAP_o$-$P_i$[k] | 1.98 | 3.01 | 99 | 3.1 | 1.98 | | 0.51, 0.54 | 1.03, 1.36 | <–150 |
| MMO–$H_o$[l] | 2.04 | 3.42 | 114 | | 2.04 | | 0.51 | 1.16 | ~–8 |

[a] Average distances and angles or ranges. Parameters for the proteins were determined from EXAFS data; angles were calculated. [b] At 4.2 K, except for Uf (80 K), BPAP (80 K), and $[Fe_3(OH)_2(O_2CPh)_4(N3)_2]^{3+}$ (250 K). [c] From temperature-dependent magnetic susceptibility (model compounds, BPAP), NMR (Uf), and EPR (MMO) studies. [d] L = $HBpz_3^-$.[31] [e] Reference 30. [f] N3 = tris(1,4-dimethylimidazol-2-yl)phosphine.[19] [g] Thundathil, R. V.; Holt, E. M.; Holt, S. L.; Watson, K. *J. Am. Chem. Soc.* **1977**, *99*, 1818–1823. Blake, A. B.; Fraser, L. B. *J. Chem. Soc., Dalton Trans.* **1975**, 193–197. Dziebkowski, C. T.; Wrobleski, J. T.; Brown, D. B. *Inorg. Chem.* **1981**, *20*, 671–678. Ansenhofer, K.; De Boer, J. J. *Recl. Trav. Chim. Pays-Bas* **1969**, *88*, 286–290. [h] Salam = *N,N'*-ethylenebis(salicylamine)(2–).[22] [i] Dipic = 2,6-pyridinedicarboxylate(2–).[21] [j] References 12, 13 (EXAFS), 8, 10 (Mössbauer), and 9, 10 (magnetic data). [k] References 5 (EXAFS) and 4 (Mössbauer and magnetic data). [l] References 14 and 78 (EPR). [m] Reference 28.

it is 2.53–2.59 Å in diphenyl phosphate and diphenylphosphinate complexes.[31,44–47,57–61]

These structural differences become even more pronounced when the tris(phosphate) complex **4** is considered. Whereas the Fe–O and Fe–N distances in **4** are normal, the Fe···P distances are fairly long (3.20–3.45 Å), as is the Fe···Fe separation (4.677(1) Å). Here, the intraligand O···O distances between the donor atoms spanning the metals are 2.55 Å, and the Fe–O–P angles are as large as 164°, with an average of 147°. Similar large angles are observed in other tris(oxyanion)-bridged complexes (Fe–O–X = 138–164°).[44,45] These angles are larger than observed for hydroxo- or oxo-bridged phosphate-bridged complexes, where Fe–O–P angles (~135°) are close to Fe–O–C angles in carboxylate-bridged complexes.[13,28,30–32,44,45,50–71] It appears that the positions of the lone pairs on the oxygen donor atoms in phosphate and chromate ligands can accommodate larger angles, perhaps because of partial $d_\pi$–$p_\pi$ mixing. Since Fe–O–C angles are not usually much greater than 140°, it is perhaps not surprising that a syn–syn tricarboxylate-bridged complex analogous to **4** has not been observed. There might not be enough room to fit more than two bidentate syn–syn carboxylate bridging ligands between two Fe(III) atoms. On the other hand, phosphate bridges probably do not allow metal atoms to be very close together, since $P–O_{Fe}$ distances are considerably longer than $C–O_{Fe}$ distances, resulting in the longer bite distances. These observations may help to explain why trinuclear $\mu_3$-oxo hexakis($\mu$-phosphato) complexes, or basic metal phosphates, have not been observed.[72] Bridging phosphate groupsmay have difficulty supporting the short M···M distances required by M–O–M angles near 120° in such triangular compounds.

Table 4 compares relevant geometric features of **1–4** with extended X-ray absorption fine structure (EXAFS) results for the phosphate derivatives of oxidized uteroferrin (Uf)[12,13] and beef spleen purple acid phosphatase, BPAP,[5] and for the hydroxylase component of methane monooxygenase (MMO-H).[14,73] The Fe–O distance in oxidized Uf phosphate, 1.94 Å, is consistent with the presence of a hydroxo bridge, but the Fe···Fe distance (3.27 Å) is shorter than observed for the hydroxo-bridged model compounds (Fe···Fe = 3.4–3.6 Å).[13] The protein may have an additional monodentate bridging group as well as a bridging phosphate ligand,[13] which would account for the shorter distance. It is likely that phosphate bridges the two iron atoms since the Fe···Fe distance lengthens when arsenate is substituted for phosphate in oxidized uteroferrin complexes.[13] An oxo-bridged phosphate-bridged core structure is eliminated by the absence of a short $Fe–O_{oxo}$ distance (~1.80 Å).[5,12,13] For methane monooxygenase, both Fe–O and Fe···Fe vectors are consistent with a hydroxo-bridged structure similar to that found in **1–3**.[14,73] In fact, the EXAFS spectra of MMO hydroxylase from *Methylococcus capsulatus* (Bath) were very similar to those of **1**,[14] and recent ENDOR results have provided evidence for a hydroxide bridge in the mixed-valent form of this protein.[15]

**Electronic and Vibrational Spectroscopy.** The optical spectra of $[Fe_2(OH)(O_2CCH_3)_2(HBpz_3)_2](ClO_4)$ (**1**), $[Fe_2(OH)\{O_2P(OC_6H_5)_2\}_2(HBpz_3)_2](BF_4)$ (**2**), and $(Fe_2\{O_2P(OC_6H_5)_2\}_3(HBpz_3)_2](BF_4)$ (**4**) are quite similar and consist entirely of charge-transfer transitions in the UV region. The orange color of the complexes is caused by the tailing of the absorption near 375 nm into the visible region. This absorption is presumably caused by a $HBpz_3^-$ ligand-to-metal charge-transfer transition, since not all hydroxobis(carboxylato)-bridged diiron(III) complexes have a band in this region.[53] Oxo-bridged diiron(III) complexes such as $[Fe_2O(O_2CCH_3)_2(HBpz_3)_2]$ (**5**)[30] have several visible absorption bands arising from charge-transfer and ligand field transitions. The optical spectra of diiron(III) centers are thus very sensitive to protonation of the oxo ligand to form a hydroxo bridge.

(59) Toney, J. H.; Brock, C. P.; Marks, T. J. *J. Am. Chem. Soc.* **1986**, *108*, 7263–7274.
(60) Kumara Swamy, K. C.; Schmid, C. G.; Day, R. O.; Holmes, R. R. *J. Am. Chem. Soc.* **1988**, *110*, 7067–7076.
(61) Colamarino, P.; Orioli, P. L.; Benzinger, W. D.; Gillman, H. D. *Inorg. Chem.* **1976**, *15*, 800–804.
(62) Betz, P.; Bino, A. *Inorg. Chim. Acta* **1988**, *147*, 109–113.
(63) Yan, S.; Que, L., Jr.; Taylor, L. F.; Anderson, O. P. *J. Am. Chem. Soc.* **1988**, *110*, 5222–5224.
(64) Murch, B. P.; Bradley, F. C.; Que, L., Jr. *J. Am. Chem. Soc.* **1986**, *108*, 5027–5028.
(65) Wieghardt, K.; Pohl, K.; Gebert, W. *Angew. Chem., Int. Ed. Engl.* **1983**, *22*, 727–728.
(66) Chaudhuri, P.; Wieghardt, K.; Nuber, B.; Weiss, J. *Angew. Chem., Int. Ed. Engl.* **1985**, *24*, 778–779.
(67) Toftlund, H.; Murray, K. S.; Zwack, P. R.; Taylor, L. F.; Anderson, O. P. *J. Chem. Soc., Chem. Commun.* **1986**, 191–193.
(68) Gomez-Romero, P.; Casan-Pastor, N.; Ben-Hussein, A.; Jameson, G. B. *J. Am. Chem. Soc.* **1988**, *110*, 1988–1990.
(69) Vincent, J. B.; Huffman, J. C.; Christou, G.; Li, Q.; Nanny, M. A.; Hendrickson, D. N.; Fong, R. H.; Fish, R. H. *J. Am. Chem. Soc.* **1988**, *110*, 6898–6900.
(70) Yan, S.; Cox, D. D.; Pearce, L. L.; Juarez-Garcia, C.; Que, L., Jr.; Zhang, J. H.; O'Connor, C. J. *Inorg. Chem.* **1989**, *28*, 2507–2509.
(71) Morris, N. L.; Ben-Hussein, A.; Jameson, G. B. *J. Inorg. Biochem.* **1989**, *36*, 263–298.
(72) Cannon, R. D.; White, R. P. *Prog. Inorg. Chem.* **1988**, *36*, 195–298.
(73) Prince, R. C.; George, G. N.; Savas, J. C.; Cramer, S. P.; Patel, R. N. *Biochim. Biophys. Acta* **1988**, *952*, 220–229.

Complexes **1–4** have no visible absorption bands, because the ligand field transitions are forbidden by orbital and spin selection rules. The strong magnetic coupling in the oxo-bridged analogues enhances the ligand field transitions, but apparently the weak coupling in **1–4** is not sufficient to produce a similar enhancement. Ligand field transitions have been discerned in the near-infrared region of the spectrum for **1** (1115 nm, 0.9 $cm^{-1}$ $M_{Fe}^{-1}$)[55] and **2** (1020 nm, 0.6 $cm^{-1}$ $M_{Fe}^{-1}$). Unlike **1–4**, the spectra of which are indistinguishable from those of mononuclear high-spin ferric complexes, $[Fe_2(OH)(O_2CCH_3)_2(TMIP)_2](ClO_4)_2(BF_4)$ and $[Fe_3(OH)_2(O_2CC_6H_5)_4(N3)_2](PF_6)_3$ do have absorbances at 440–480 nm ($\epsilon$ 225–260 $cm^{-1}$ $M_{Fe}^{-1}$),[18,19] values similar to those of the ligand field transitions occurring in the oxo-bridged complexes.[31,74-76] There is evidence that the linear trinuclear complex $[Fe_3(OH)_2(O_2CC_6H_5)_4(N3)_2](PF_6)_3$ is more strongly antiferromagnetically coupled than the dinuclear complexes, which may help to explain the intensities of the transitions at 440–480 nm.[19] Comparison of the UV spectra of **1–3** with those of their oxo-bridged analogues suggests that carboxylate (or phosphate) → Fe(III) transitions occur near 260 nm (38 500 $cm^{-1}$), $\mu$-oxo → Fe(III) transitions at 310–340 nm (29 400–32 000 $cm^{-1}$), and pz → Fe(III) transitions near 360 nm (27 800 $cm^{-1}$).[31,74-76] The $\mu$-OH → Fe(III) transitions cannot be identified, and they may fall under the carboxylate and phosphate LMCT bands.

**Mössbauer Spectra.** The $^{57}Fe$ Mössbauer spectra for $[Fe_2(OH)(O_2CCH_3)_2(HBpz_3)_2](ClO_4)$ (**1**), $[Fe_2(OH)\{O_2P(OC_6H_5)_2\}_2(HBpz_3)_2](BF_4)$ (**2**), and $[Fe_2(OH)\{O_2P(C_6H_5)_2\}_2(HBpz_3)_2](BF_4)$ (**3**) are shown in Figure S1. Mössbauer parameters are presented together with those of purple acid phosphates, the oxidized hydroxylase protein of methane monooxygenase, and selected model compounds in Table 4. Isomer shifts all fall between 0.4 and 0.6 mm/s, typical of high-spin ferric ion in this environment,[17] but the quadrupole splitting values for the hydroxo-bridged complexes are very small (0.2–0.4 mm/s) compared to those of other ferric complexes. In particular, the $\Delta E_Q$ values for **1–3** are markedly different from those of their oxo-bridged analogues (~1.6 mm/s). Quadrupolar coupling constants are related to the anisotropy in the electric field gradient around the iron atom, from which it appears that the electric field in the hydroxo-bridged complexes is relatively isotropic. From this information we conclude that dinuclear iron(III) centers are unlikely to be bridged by oxo ligands if their quadrupolar coupling constants are substantially lower than 1 mm/s but that larger $\Delta E_Q$ values provide little insight into the nature of the monoatomic bridge. The quadrupole coupling parameters for oxidized methane monooxygenase hydroxylase and the phosphate-bound forms of uteroferrin and beef spleen phosphatase (1.0–1.4 mm/s), which are unlikely to contain oxo bridges on the basis of EXAFS and other data,[4,8,12-14,73,77-81] indicate somewhat more anisotropy in the electric field gradient of the iron sites than in **1–3**.

**Magnetic Susceptibility.** Magnetic susceptibility data for powdered **1–3** are shown in Figure 2. It was not possible to fit these data well with a simple expression for an antiferromagnetic exchange coupling constant, $J$, and a paramagnetic impurity term, $p$, using the spin-exchange Hamiltonian $H = -2JS_1 \cdot S_2$.[50] Fits were therefore attempted for expressions allowing for temperature-independent paramagnetism, a $g$-value other than 2, a Weiss parameter ($\Theta$),[50] the molecular field approximation, or a biquadratic exchange mechanism.[41-43] None of these expressions yielded satisfactory fits. With these difficulties, we obtained $J$ values on the order of –15 $cm^{-1}$ for **1–3** from the usual fitting procedures.[50] The field dependence of the susceptibilities of **1** and **2** was investigated at various temperatures and found to vary linearly up to a field of at least 50 kG.

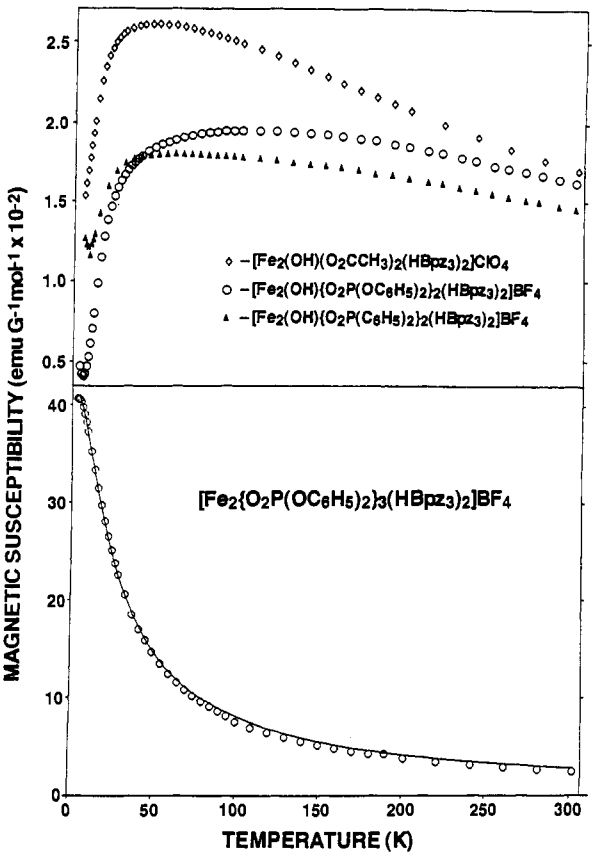


**Figure 2.** Plots of solid-state magnetic susceptibility versus temperature (top) for powdered hydroxo-bridged complexes and (bottom) for powdered $[Fe_2\{O_2P(OC_6H_5)_2\}_3(HBpz_3)_2](BF_4)$, **4**, including (solid line) the fit described in the text.

Also shown in Figure 2 are the solid-state magnetic susceptibility data for $[Fe_2\{O_2P(OC_6H_5)_2\}_3(HBpz_3)_2](BF_4)$, **4**, which were fit reasonably well by allowing $J$ and $p$ to vary, although slightly better fits were obtained by allowing $g$ to vary and not including a paramagnetic impurity term. The fit shown is for $J$ = –0.8(1) $cm^{-1}$ and fixing $g$ = 2.0 and $p$ = 0. This antiferromagnetic coupling interaction is weaker than that of $[Fe_2(O_3POC_6H_5)_3(metacn)_2]$ ($J$ = –3.5(2) $cm^{-1}$) and $[Fe_2(HPO_4)_3(metacn)_2]$ ($J$ = –2.9(6) $cm^{-1}$) but similar to that of $[Fe_2(HAsO_4)_3(metacn)_2]$ ($J$ = –1.0(2) $cm^{-1}$), where metacn = 1,4,7-trimethyl-1,4,7-triazacyclononane.[44,45]

The effective magnetic moments per iron of **1**, **3**, and **4** in the solid state, 4.36 $\mu_B$ (300 K), 4.53 $\mu_B$ (302 K), and 5.44 $\mu_B$ (281 K), agree approximately with the values of 4.4 $\mu_B$ (300 K), 4.8 $\mu_B$ (293 K), and 5.7 $\mu_B$ (293 K), respectively, measured in $CD_2Cl_2$ solution, consistent with retention of the bridged structures for the complexes in solution.

Antiferromagnetic exchange coupling constants of $J$ < –40 $cm^{-1}$ and $J$ < –150 $cm^{-1}$ have been estimated for uteroferrin and beef spleen phosphatase, respectively.[5,12] From these values, it appears that the iron atoms in the proteins are fairly strongly coupled to one another, although the relatively long Fe–O distances found from EXAFS experiments of *ca.* 1.94 Å[5,12,13] suggest that

(74) Reem, R. C.; McCormick, J. M.; Richardson, D. E.; Devlin, F. J.; Stephens, P. J.; Musselman, R. L.; Solomon, E. I. *J. Am. Chem. Soc.* **1989**, *111*, 4688–4704.
(75) Sanders-Loehr, J.; Wheeler, W. D.; Shiemke, A. K.; Averill, B. A.; Loehr, T. M. *J. Am. Chem. Soc.* **1989**, *111*, 8084–8093.
(76) Sanders-Loehr, J. In *Iron Carriers and Iron Proteins*; T. M. Loehr, Ed.; VCS Publishers: New York, 1989; pp 373–466.
(77) Woodland, M. P.; Dalton, H. *J. Biol. Chem.* **1984**, *259*, 53–59.
(78) Fox, B. G.; Hendrich, M. P.; Surerus, K. K.; Andersson, K. K.; Froland, W. A.; Lipscomb, J. D.; Münck, E. *J. Am. Chem. Soc.* **1993**, *115*, 3688–3701.
(79) Fox, B. G.; Froland, W. A.; Dege, J. E.; Lipscomb, J. D. *J. Biol. Chem.* **1989**, *264*, 10023–10033.
(80) Fox, B. G.; Surerus, K. K.; Münck, E.; Lipscomb, J. D. *J. Biol. Chem.* **1988**, *263*, 10553–10556.
(81) Ericson, A.; Hedman, B.; Hodgson, K. O.; Green, J.; Dalton, H.; Bentsen, J. G.; Beer, R. H.; Lippard, S. J. *J. Am. Chem. Soc.* **1988**, *110*, 2330–2332.

**Table 5.** Summary of NMR Results for **1–4**

| | shift, ppm ($T_1$, ms) | | | |
|---|---|---|---|---|
| assgnt | 1 | 2 | 3 | 4 |
| 4(5)-pz[a] | 61 | 62 (≤0.04) | 64 (≤0.04) | 100 |
| 5(4)-$pz_{cis}$[a] | 37 | 37 (0.16) | 41 (0.18) | 50 |
| 5(4)-$pz_{trans}$[a] | 28 | 29 (0.16) | 36 (0.18) | 50 |
| 3-pz | ~16 | ~9 (≤0.04) | ~14 (0.2) | 32 |
| Ph | [69][b] | 8.3 (0.6) | 13.0 (0.7) | 8.4 |
| Ph | | 8.1 (0.6) | 12.0 (0.6) | |
| Ph | | 7.2 (1.5) | 6.7 (1.0) | 6.8 |
| Ph | | 7.1 (1.0) | 6.0 (1.5) | |
| Ph | | 1.7 | 1.7 | 1.7 |
| B–H | −14 | −14 (≤0.04) | −14 (≤0.04) | −20 |

[a] Either 4-pz or 5-pz. [b] $CH_3COO^-$.

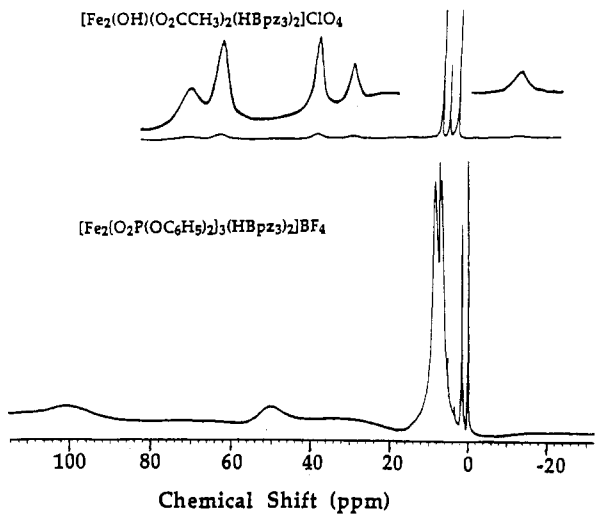


**Figure 3.** Representative $^1H$ NMR spectra in $CD_2Cl_2$ or $CDCl_3$ solution.

the extent of coupling should be similar to that found in the hydroxo-bridged complexes **1–3**. A $J$ value of −32 $cm^{-1}$ was observed for the semireduced hydroxylase of MMO; the value for the oxidized protein was recently estimated to be −8 ± 3 $cm^{-1}$.[14,78]

**NMR and EPR Spectra.** The $^1H$ NMR spectra of **1–4** are representative of weakly coupled, high-spin diiron(III) complexes. Assignments of the resonances, summarized in Table 5 and shown for **1** and **4** in Figure 3, were made by comparing results for the complexes with one another, with the spectra of oxo-bridged analogues,[31] and with those of more weakly coupled diiron(III) complexes,[82,83] as well as by NMR $T_1$ measurements. The hydroxo-bridged complexes **1–3** have $^1H$ NMR resonances that are very similar to each other, but which are considerably more shifted (−20 to +80 ppm) than those of their oxo-bridged analogues (2–16 ppm). The spectrum of $[Fe_2\{O_2P(OC_6H_5)_2\}_3(HBpz_3)_2](BF_4)$ (**4**) is like those of the hydroxo-bridged complexes, but the observed chemical shift range is larger (−20 to +110 ppm).

Resonances of protons on the hydrotris(1-pyrazolyl)borate ligands are the most shifted and broadened. The pyrazole proton resonances exhibit relaxation times of less than 0.2 ms. Up to six pyrazole proton resonances are expected, one for each of the ring protons in positions anti or syn to the hydroxo bridge. Since protons as close to the metal atoms as the pyrazole protons in the 3-position are expected to be very broad,[31,82,83] the sharper downfield resonances probably arise from hydrogens in the 4- and 5-positions. The peaks at 61–64 ppm in **1–3**, and at 100 and 50 ppm in **4**, which integrate to 6 protons each, are assigned to pyrazole ring protons in either the 4- or 5-position, the syn and anti resonances of which overlap. The syn and anti resonances,

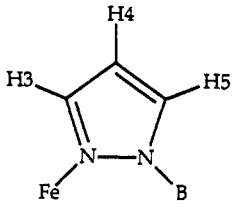


respectively, of the other proton are resolved at 37–41 ppm (4 protons), and 36–38 ppm (2 protons) in **1–3**. Very broad peaks are observed in the spectra of **1–4** at 9–30 ppm (see Table 5), which may be due to protons in the 3-positions. The resonances at ~−14 ppm in **1–4**, with areas corresponding to 2 protons each and spin–lattice relaxation times of less than 0.04 ms, may then be assigned to the B–H protons.

$^{31}P$ NMR spectra of **2** and **3** were measured (4000 ppm range; 15 000 scans), but a phosphorus signal was not observed, suggesting that the nuclear spin relaxes too quickly to be detected. Phosphate-bound oxidized purple acid phosphatase does not have an observable $^{31}P$ NMR signal either, nor do the oxo-bridged analogues of **2** and **3**.[4,31]

EPR spectra of **1–3** are shown in Figure S2, and peak positions are listed in the Experimental Section. A number of fairly strong signals are observed for the hydroxo-bridged complexes at 4–78 K. The overall signal appears to be stronger at low temperatures, but more structure is detected at higher temperatures. A feature at $g \sim 4.3$ in the complexes is probably due to a small amount of a mononuclear high-spin iron(III) impurity. Significantly, the strongest signals for **2** and **3** (4–25 K) have $g$-values of less than 2, 1.89, and 1.91, respectively, and a similar, weaker signal is observed for **1** at $g = 1.83$ (78 K). The low-field signals in **2** and **3** ($g \geq 14$) become more intense at higher temperature, as expected for transitions between excited states which are more populated as the temperature increases. EPR spectra of the diiron(III) form of the hydroxylase of methane monooxygenase have small signals near $g = 4.3$ for iron(III) and near $g = 2.0$ for organic radicals,[14,79] as well as a sharp resonance at $g = 8.0$ that is enhanced in parallel field.[78] A small amount of semireduced MMO hydroxylase, with signals at $g = 1.94$, 1.86, and 1.75, may also be observed.[14,77,79]

## Concluding Remarks

Complexes containing a phosphate- or acetate-bridged ($\mu$-hydroxo)diiron(III) core, such as may exist in the metalloproteins uteroferrin, beef spleen purple acid phosphatase, and the hydroxylase component of methane monooxygenase, have been prepared. The core in these complexes is expanded relative to $\mu$-oxo analogues, decreasing the magnitude of the antiferromagnetic spin exchange coupling constants and affording correspondingly larger paramagnetic shifts in the $^1H$ NMR spectra of the hydroxo-bridged complexes. These results further demonstrate the potential for the magnetic parameters of iron oxo proteins to afford useful information about the chemical constitution of their cores. Electronic transitions are very different from those of oxo-bridged complexes. None of the intensity-enhanced d–d transitions of the latter are observed, indicating that the weak antiferromagnetic coupling in the hydroxo-bridged complexes is not sufficient for relaxation of the spin selection rule. Mössbauer quadrupolar coupling parameters are characteristically small in the hydroxo-bridged complexes.

Comparisons of the spectroscopic and structural features of the model complexes with those of oxidized uteroferrin phosphate are not inconsistent with the conclusion that a hydroxo-bridged diiron(III) center is present in this protein.[5,12,13] For the hydroxylase of methane monooxygenase, there is a similarity between the cores based on EXAFS studies, and the UV and EPR spectroscopic data as well as the magnetic exchange coupling constant results are consistent with a hydroxo-bridged struc-

(82) Wu, F.-J.; Kurtz, D. M., Jr. *J. Am. Chem. Soc.* **1989**, *111*, 6563–6572.
(83) Arafa, I. M.; Goff, H. M.; David, S. S.; Murch, B. P.; Que, L., Jr. *Inorg. Chem.* **1987**, *26*, 2779–2784.

ture.[15,78] The Mössbauer quadrupolar coupling parameters are less diagnostic of such a unit, however.

**Acknowledgment.** This work was supported by U.S. Public Health Service Grant GM-32134 from the National Institute of General Medical Sciences (S.J.L.) and Training Grant CA-09112 of the National Institutes of Health (P.N.T., W.H.A.). We also wish to thank Dr. G. C. Papaefthymiou of the Francis Bitter National Laboratory for Mössbauer studies and are grateful for the assistance of Drs. R. L. Rardin, R. H. Beer, and J. G. Bentsen.

**Supplementary Material Available:** Tables S1–S12, listing final positional and thermal parameters and complete bond distances and angles for **1–4**, and Figures S1 and S2, showing Mössbauer and EPR data, respectively (43 pages). Ordering information is given on any current masthead page.